Probing Interfacial Co-Crystallisation using Simultaneous Potential and Current Measurements at Liquid-Liquid Interfaces Polarised by Common Ion Approach

Magdalena Kaliszczak, Imane Bamou, Marina Garcia-Atance, Franca Jones, Damien Arrigan, Grégoire Herzog

Probing Interfacial Co-Crystallisation using Simultaneous Potential and Current Measurements at Liquid-Liquid Interfaces Polarised by Common Ion Approach

Magdalena Kaliszczak,[1] Imane Bamou,[1] Marina Garcia-Atance,[1] Dr Franca Jones,[2] Prof Dr Damien WM Arrigan,[2] Dr Grégoire Herzog[1,*]

[1]: Université de Lorraine, CNRS, LCPME, F-54000 Nancy, France

[2]: School of Molecular and Life Sciences, Curtin University, GPO Box U1987, Perth, Western Australia 6845, Australia

E: gregoire.herzog@cnrs.fr

Abstract

The simultaneous measurement of potential and current variations at the interface between two immiscible electrolyte solutions, which were polarised using tetraalkylammonium cations as a common ion, is reported here. Various concentration ratios of tetramethyl-, tetraethyl-, and tetrapropylammonium were dissolved in both phases. Such biphasic systems were then used to verify that the interfacial potential difference measured fit the theoretical calculations. This experimental set-up was then used to probe the interfacial cocrystallisation process of hydrophilic and cationic caffeine with lipophilic 1-hydroxy-2-naphtoic acid (1H2N). The presence of caffeine in the aqueous phase led to higher current values, caused by interfacial charge transfer. Electrochemical noise analysis suggested that a two-step process was occurring at the ITIES with (i) a potential-driven nucleation with the tranfer of caffeine from the aqueous to the organic phase; (ii) a growth stage where the interfacial potential does no longer play a role.

Introduction

In recent years, the liquid-liquid interface has been used as a tool to control the formation of different types of assemblies e.g. supramolecular[1], gold nanoparticles[2][3], phospholipids,[4] mesoporous silica[5], porphyrin[6][7], proteins[8] and polyamides[9]. When the interface is electrochemically polarised, it is a powerful tool to observe the transfer of charge (ions and/or electrons) by following the changes in current. These charge transfers are induced by the application of a Galvani potential difference across the interface[10]. The potential difference between two immiscible electrolyte solutions (ITIES) can be controlled by either a four-electrode potentiostat[11] or by the dissolution of a common ion in each phase as described by the Nernst-like equation:

$$\Delta_o^w\Phi = \Delta_o^w\Phi_i^0 + \frac{RT}{z_iF} ln \frac{c_i^o}{c_i^w} \quad (1)$$

Where $\Delta_o^w\Phi$ – the Galvani potential difference; $\Delta_o^w\Phi_i^0$ – standard transfer potential of the ion i; z_i – charge of ion i; c_i – concentration in each phase.

When $\Delta_o^w\Phi$ is imposed by a potentiostat, the concentration ration of species *i* is modified according to equation (1)[12]. In the case of the common ion approach, $\Delta_o^w\Phi$ is set by the concentration of a common species, *i*, in each phase.[13] The undeniable advantage of using common ion experiments is the greater possibility of approaching realistic conditions and the possibility of creating biomimetic systems. These are also known as 'shake flasks' experiments that enable analyses difficult to perform using a potentiostat, such as liquid-liquid extraction[14], the study of interfacial ion distribution[15], monitoring electrodeposition at the ITIES[16] or biomimetic reduction of oxygen[17]. However, when the interface is polarised by the common ion approach, monitoring the potential and the current associated with any chemical reactions is challenging. Such reactions can be followed visually[18,19] and by the use of analytical methods (e.g. UV-vis absorption spectroscopy). Recently, potential changes at the ITIES have been monitored by open circuit potential (OCP) measurements and concentrations were calculated based on the Nernst-like equation shown as Eq. (1). The extraction of tetraalkylammonium chloride salts from an aqueous phase to the organic phase (1,2-dichloroethane, DCE) was explained by examining the OCP at the water/DCE interface[20–22]. Current changes occurring in emulsions on the ITIES were also followed using chronoamperometry[23]. Current spikes associated with single microdroplets fusion events at the polarised interface were detected and quantitatively analysed. The number of ions present

in a single droplet was calculated directly from the charge of the corresponding spike. Yet, this method focused only on current analysis – a separate study of single fusion events through OCP was later reported.[24]

Electrochemical noise (EN) is a method commonly used, which allows the simultaneous measurement of spontaneous variation of potential and current caused by corrosion events.[25,26] Indeed, most semi-macroscopic phenomena associated with corrosion are stochastic, which make their study difficult by electrochemical impedance spectroscopy or polarisation curves. Potential electrochemical noise, δE, represents the variation of potential around a dc potential value, whereas current electrochemical noise, δI, is the stochastic variation of current around a dc current value. These variations, δE and δI, can be analysed in the time domain based on different parameters such as the shape, amplitude and frequency. Analysis can also be made in the frequency domain by the calculation of the power spectral density of the current and potential fluctuations[26]. Electrochemical noise allows thus to determine corrosion rates and to identify different corrosion events: e.g. (i) monitoring of the formation and destruction of corrosion inhibitor films[27], investigating the mechanism of formation of the lithium-based conversion layer[28] or analysing aqueous corrosion inhibition process[29]. Simultaneous measurements of potential and current fluctuation is possible thanks to a zero resistance ammeter[30].

We propose here to monitor simultaneously current and potential changes associated with cocrystallisation events at a liquid-liquid interface polarised by a common ion dissolved in each phase. Polarised liquid-liquid interfaces have recently been used to produce cocrystals of caffeine and 1-hydroxy-2-naphthoic acid[31]. XRD analysis of the cocrystals showed two crystallographic phases. These phases were formed under specific conditions: there is a majority of phase I when the interface was positively polarised; a majority of phase II in the case of a non-polarised interface, this is the natural potential of the cell. We proposed the mechanism of cocrystallisation: in case of positive polarization, the caffeine transfers to the organic phase and the cocrystals are created in the organic side of the interface. However, when no potential is applied the cocrystals are formed in an interfacial process. In order to determine the role of the interfacial potential in the cocrystallisation process, simultaneous measurement of both potential and current at the ITIES may provide important information. The electrochemical cells were assembled with various concentrations of tetraalkylammonium cations (TAA^+) in the organic and aqueous phases and the potential and current were tracked by the adaptation of the EN method to the ITIES. The electrochemical noise data were analysed

based on several parameters used in corrosion studies: the power spectral density (PSD) plots, the current root mean square (I_{rms}) values of PSD of current and the low frequency noise impedance R_{sn}. This approach provides a new way to monitor and understand events at the ITIES.

Experimental section

Chemical reagents: The aqueous phase electrolyte was lithium chloride (LiCl, Sigma Aldrich, ≥ 99%) and was used as received. The studied quaternary ammonium salts: tetrapropylammonium chloride (TPA^+Cl^-, Sigma-Aldrich, 98%), tetraethylammonium chloride (TEA^+Cl^-, Sigma-Aldrich, ≥ 98%) and tetramethylammonium chloride (TMA^+Cl^-, Sigma-Aldrich, 98%) were dissolved in the aqueous phase electrolyte. The organic phase electrolytes consisting of quaternary ammonium tetrakis (4-chlorophenyl) borate (TAA^+TPBCl^-) salts were prepared *via* metathesis reaction of tetramethyl (TMA^+Cl^-), tetraethyl (TEA^+Cl^-) and tetrapropyl (TPA^+Cl^-) ammonium chloride and potassium tetrakis (4-chlorophenylborate) (KTPBCl, 98% Aldrich). The organic phase solvent was 1,2-dichloroethane (DCE, 99% Sigma-Aldrich) and was used as received. Caffeine (laboratory reagent grade) was purchased from Fischer Scientific and 1-hydroxy-2-naphthoic acid (99%) from Aldrich. The pH of aqueous solutions was adjusted by hydrochloric acid (HCl, Honeywell, Fluka, ACS reagent, ≥ 37 %) and lithium hydroxide (LiOH, analytical reagent, Prolabo). Purified water with a resistivity of 18.2 MΩ cm (Ultrapure device from Elga Purelab) was used for preparation of aqueous solutions. Ag/AgCl reference electrodes were made *via* silver wire oxidation in a $FeCl_3$ solution. All other reagents and solvents used were analytical reagent grade.

Electrochemical experiments: The Electrochemical Noise (EN) technique was applied to measure the potential and the current synchronously. EN is usually used in the corrosion studies[32] however here it was applied to four-electrodes system at the liquid/liquid interface. The potentiostat VSP-300 Biologic (Electrochemical Applications/Corrosion) was used to measure the electrochemical potential and current noise.

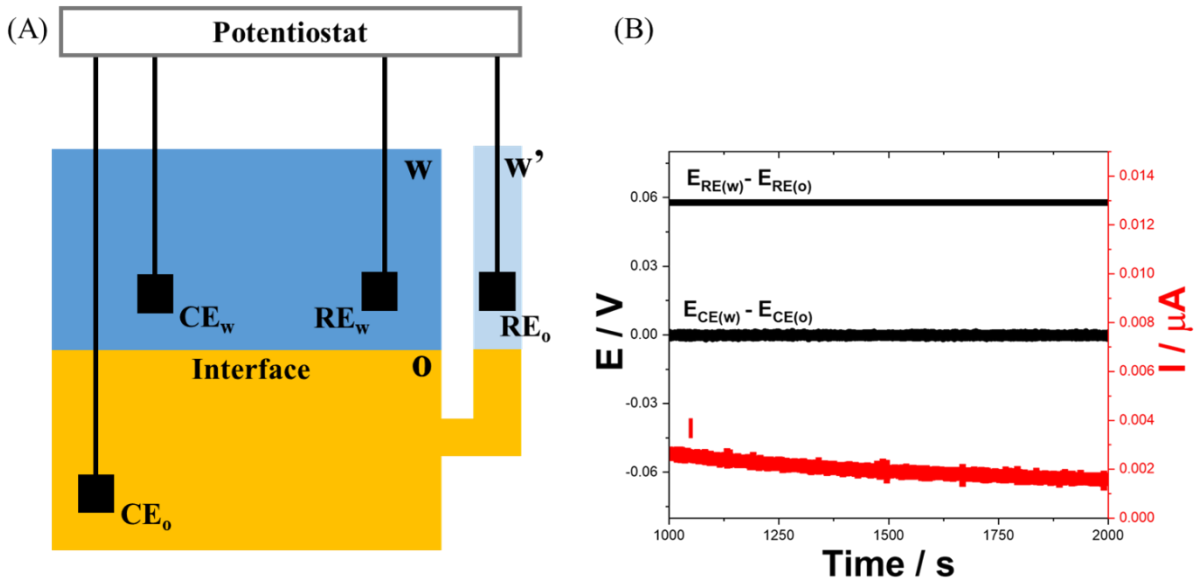

Figure 1: (A) Schematic representation of the electrochemical cell used for the simultaneous current and potential measurements. CE: counter electrode, RE: Reference electrode, o: organic phase, and w: aqueous phase. (B) Simultaneous potential (black) and current (red) measurement as a function of time. $E_{RE(w)} - E_{RE(o)}$ represents the potential measured between the two reference electrodes and $E_{CE(w)} - E_{CE(o)}$ shows the potential of 0 V (Mean ± SD: -0.00028±.00033V) imposed between the two counter electrodes. I is the current measured through the electrochemical cell.

It allows the application of 0 V between the counter electrodes in the organic phase (CE_o) and in the aqueous phase (CE_w) [26]. The potential is measured between the RE_w and REo and the current between CE_w and CE_o (Figure 1). The electrochemical cells were placed in a grounded Faraday cage.

The equilibrium potential differences at the Ag ($RE_{w'}$)/w, w/o, o/w' and w'/Ag (RE_w) interfaces can be described by the corresponding Nernst equations:

$$\Delta E = \phi_{Ag/AgCl} - \phi_{Ag/AgCl'} = \Delta_w^{Ag/AgCl}\phi + \Delta_o^w\phi - \Delta_o^{w'}\phi - \Delta_{w'}^{Ag/AgCl'}\phi \quad (2)$$

Where the different potentials are defined as follows:

$$\Delta_w^{Ag/AgCl}\phi = \Delta_w^{Ag/AgCl}\phi^0 + \frac{RT}{F} ln \frac{1}{c_{Cl-}^w} \quad (3)$$

$$\Delta_{w'}^{Ag/AgCl'}\phi = \Delta_{w'}^{Ag/AgCl}\phi^0 + \frac{RT}{F} ln \frac{1}{c_{Cl-}^{w'}} \quad (4)$$

$$\Delta_o^w\phi = \Delta_o^w\phi_{TAA^+}^0 + \frac{RT}{F} ln \frac{c_{TAA^+}^o}{c_{TAA^+}^w} \quad (5)$$

$$\Delta_o^{w'}\phi = \Delta_o^{w'}\phi_{TAA^+}^0 + \frac{RT}{F} ln \frac{c_{TAA^+}^o}{c_{TAA^+}^{w'}} \quad (6)$$

where $c^{w}_{TAA^+}$, $c^{o}_{TAA^+}$, $c^{w'}_{TAA^+}$ represents the concentration of TAA^+ in the aqueous phase, organic phase and aqueous phase for organic reference electrode, respectively, $c^{w}_{Cl^-}$, $c^{w'}_{Cl^-}$ represent the concentration of Cl^- in the aqueous phase and aqueous phase for organic reference electrode and $\Delta^{w}_{o}\phi^{o'}_{TAA^+}$ is the formal ion transfer potential difference for TAA^+.

By combining equations (2) and (3-6):

$$\Delta E = \frac{RT}{F} ln \frac{c^{w'}_{Cl^-}}{c^{w}_{Cl^-}} + \frac{RT}{F} (\ln \frac{c^{o}_{TAA^+}}{c^{w}_{TAA^+}} - ln \frac{c^{o}_{TAA^+}}{c^{w'}_{TAA^+}}) \quad (7)$$

To simplify this equation, if we keep $[c^{w}_{Cl^-} = c^{w'}_{Cl^-}]$ and that $[c^{o}_{TAA^+} = c^{w'}_{TAA^+}]$ in which case the potential measured will depend solely on $\frac{c^{o}_{TAA^+}}{c^{w}_{TAA^+}}$.

$$\Delta E = \frac{RT}{F} \ln \frac{c^{o}_{TAA^+}}{c^{w}_{TAA^+}} \quad (8)$$

This is true if[20]:

$$\Delta^{w}_{o}\phi^{0'}_{TAA^+} - \Delta^{w}_{o}\phi^{0'}_{Cl^-} \gg \frac{RT}{F} ln[4 \frac{c^{w}_{TAA^+}}{c^{o}_{TAA^+}} \left(1 + \frac{c^{w}_{TAA^+}}{c^{o}_{TAA^+}}\right)] \quad (9)$$

Based on the above-mentioned equations (Eq. 7-9) the four-electrode cell comprising liquid/liquid interface was prepared according to Scheme 1:

Scheme 1: Description of the electrochemical cells used

Electrochemical cell:	**Ref 1:**	**(w)**	**(o)**	**(w')**	**Ref 2:**	**Information:**
1	Ag/AgCl	1 mM TAACl 9 mM LiCl	x mM TAATPBCl	x mM TAACl (10 – x) mM LiCl	AgCl/Ag	x = 0.1, 0.5, 1, 5, 10
2	Ag/AgCl	X 0.01 mM TMACl	Y 10 mM TMATPBCl	10 mM TMACl 10 mM LiCl	AgCl/Ag	X = -, Caff SAT Y = -, 1H2N

		9.995 mM LiCl 9.995 mM HCl					
3	Ag/AgCl	X mM Caff x mM TMACl 10-(x/2) mM LiCl 10-(x/2) mM HCl	10 mM 1H2N y mM TMATPBCl	Y mM TMACl 20 – y mM LiCl	AgCl/Ag	X = 40, SAT x = 0.01, 0.1, 1, 10 y = 0.01, 0.1, 1, 10	

The volumes of the aqueous (w) and organic (o) phases were both 2.5 mL. The surface area of the interface was 1.13 cm^2. The delay between the preparation of the cells and the start of the experiment was 45 s. The same time was kept in each experiment to allow comparison between experiments. The measurements were carried out for 60 min to allow the electrochemical cell to reach equilibrium. The change in potential and current is a result of ions transferring at the liquid/liquid interface and allows changes on the interface to be followed during the establishment of equilibrium at this interface. The potential and the current were recorded at room temperature every 0.01 s, sufficiently frequent to observe current and potential spikes.

Since EN has been employed to monitor the type of corrosion and find the corrosion rate, in this work we have used similar parameters to explain the processes taking place at the phase interface. The recorded experimental potential and current data were then used to analyse the electrochemical noise via Microsoft Excel.[33] Power spectral density (PSD) in the frequency domain is used to predict the corrosion mechanism and can be used to compare processes taking place at the ITIES. Our data have a large number of points and repeated signals, so PSD plots can be calculated using Fast Fourier Transform (FFT).

Before the results could be analysed, the baseline had to be removed. This was done using Origin® software and the polynomial removal procedure. To do this, we constructed graphs of

potential or current over time, adding the trend line that provides the best fit to the data. The results were divided into ten sections of 20 seconds each, consisting of exactly 2048 points. In these time sections, PSD_E and PSD_I in the frequency domains were calculated. In this work, the equation 10 is used to calculate the PSD:

$$PSD_x(f) = |X_T(f)|^2 = \left[Re\left(X_T(f)\right)\right]^2 + \left[Im\left(X_T(f)\right)\right]^2 \quad (10)$$

Where $X_T(f)$ is the Fourier transform of x(t), T is the experimental time, Re and Im correspond to real and imaginary part, respectively and the number 2 means that only positive frequencies are concerned.[33]

Root mean square current (I_{rms}) was calculated using Eq. (11) as the ratio of standard deviation of current PSD (PSD_I).

$$I_{rms} = \sqrt{\frac{\sum_i^n PSD_I}{n}} \quad (11)$$

Where n was the number of experimental data points.

The low frequency noise impedance (R_{sn}) was determined as the ratio of the standard deviations of experimental potential (δΔE) and current (δI) after the baseline removal (Eq. 12) .[25,28]

$$R_{sn} = \left|\frac{PSD_E(f)}{PSD_I(f)}\right|^{\frac{1}{2}} \quad (12)$$

Where$PSD_E(f)$ and $PSD_I(f)$ are the power spectral density of the potential ΔE, and the current density (I), respectively, in the frequency domain f.

Results and Discussion

Measurement of the potential difference:

A first series of experiments was designed to check that the potential measured is consistent with the potential expected from equation (8). Several configurations of electrochemical cell (1) were prepared with the different ratio of tetralkylammonium (TAA^+) in organic and aqueous phase.

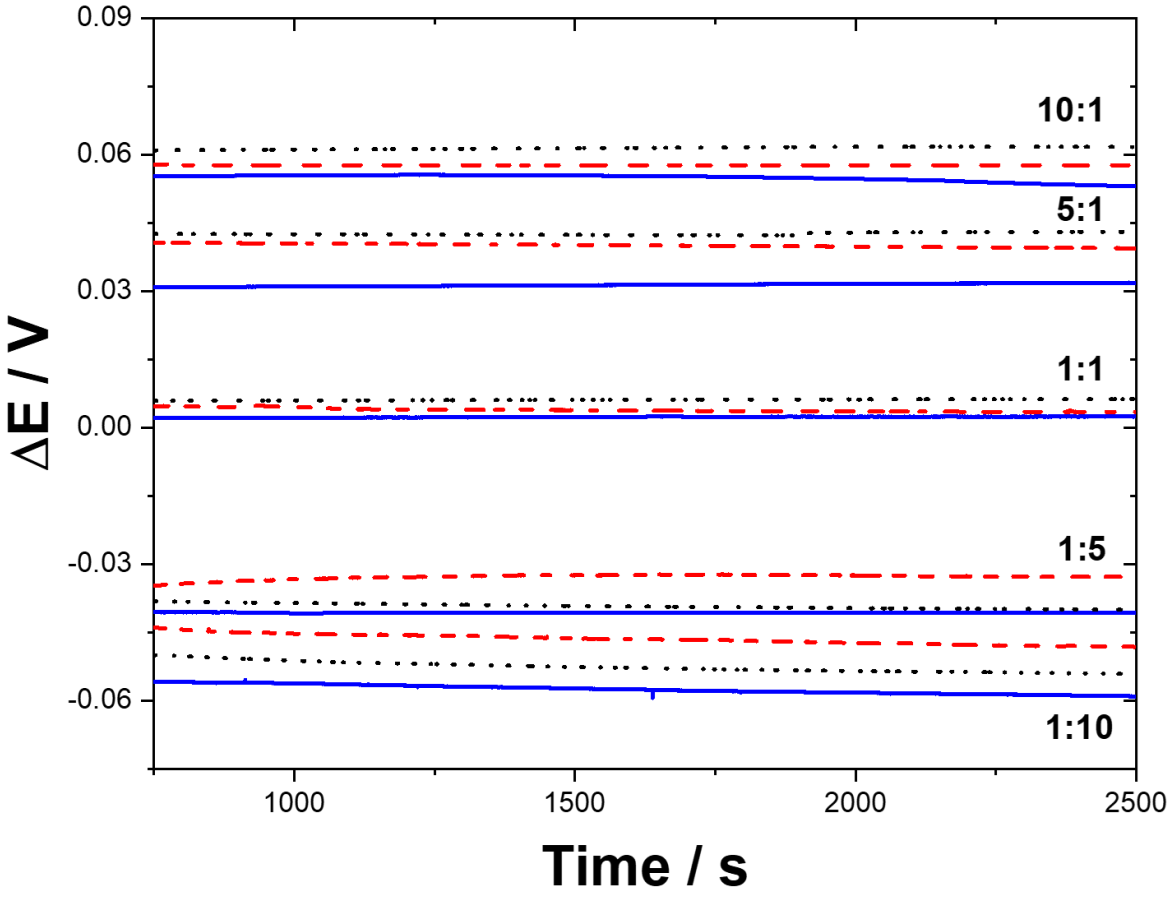

Figure 2: Change of potential as a function of time in the various configurations according to cell 1 Table 1. TMA^+ (···), TEA^+ (---) and TPA^+ (——). The presented ratio corresponds to $\frac{c^o_{TAA^+}}{c^w_{TAA^+}}$ ratio.

In these experiments, the interface is polarised by the distribution of a common TAA^+ ion between the two immiscible phases. The measurements were performed for 1 hour to allow the partition of ions to reach equilibrium at the liquid/liquid interface. The measurements were started right after the electrochemical cells where prepared. The comparison of the change of the potentials in time for three TAA^+ (TMA^+, TEA^+ and TPA^+) and various ratios of concentration in organic and in aqueous phase is shown in Figure 2. The potential is stable in time and its value decreases with the $\frac{c^o_{TAA^+}}{c^w_{TAA^+}}$ ratio. Similar results were obtained for the three ions, TMA^+, TEA^+ and TPA^+, which indicated that the transfer is not based on the formal transfer potential, but on the ratio of concentration of TAA^+ in each phase, as expected from equation (8).

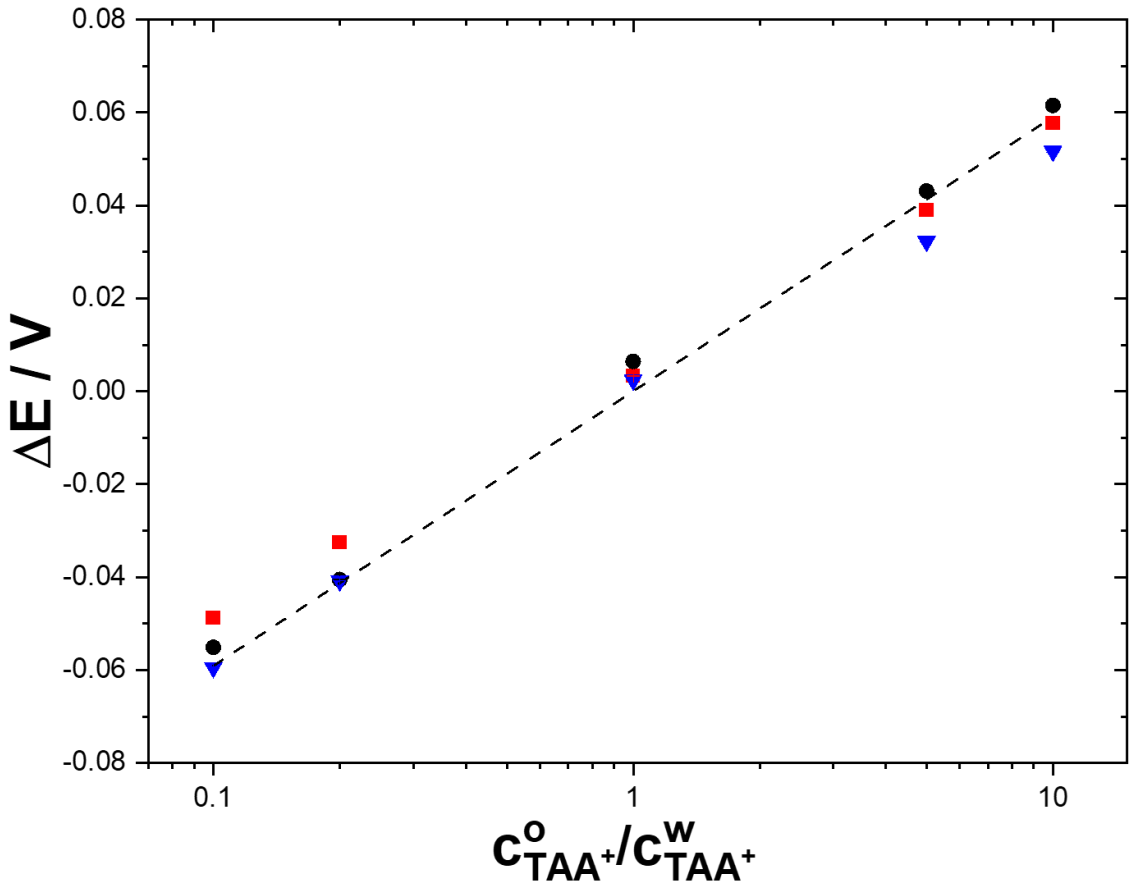

Figure 3: Equilibrium potential dependences on the ratio of common ion in organic and aqueous phases $\frac{c^o_{TAA^+}}{c^w_{TAA^+}}$. TMA^+ (●), TEA^+ (■) and TPA^+ (▼). Dashed line represents theoretical data calculated according to Eq. (8). When not visible, error bars are smaller than symbols.

In Figure 3, we see the dependence of the potential on the ratio of the concentrations in the organic and aqueous phases. The dashed line and crosses represent the theoretical calculations based on Eq. (9). We see that the three cations, TMA^+, TEA^+ and TPA^+, fit into the theoretical calculations. When the ratio is 1:1, the potential is around 0 V (Mean±SD: 3.3±0.06mV, 6.4±0.02mV, 2.39±0.02mV for TMA^+, TEA^+ and TPA^+ respectively). This confirms compliance with theoretical assumptions. The potential is positive when there is the excess of the ion in the organic phase and it takes negative values when the concentration in the aqueous phase is higher than in the organic phase. The potentials for the cells built with these three quaternary ammonium salts are very close to the theoretical values calculated (Figure 3) confirming that this method is suitable to monitor the changes of potential at the ITIES. The difference between the theoretical calculations (based on the Eq. 8) and experimental results

might originate from the moisture content of the TAACl salts or impurities from the self-prepared TAATPBCl salts or small difference in the reference electrodes.

Simultaneous measurement of potential and current:

In the next part of the study, along with the well-defined solutions which comply with theory (Figures 2 and 3), we set up the electrochemical cell with saturated solution of caffeine as the aqueous phase and 1-hydroxy-2-naphthoic acid to the organic phase, according to electrochemical cell 2.

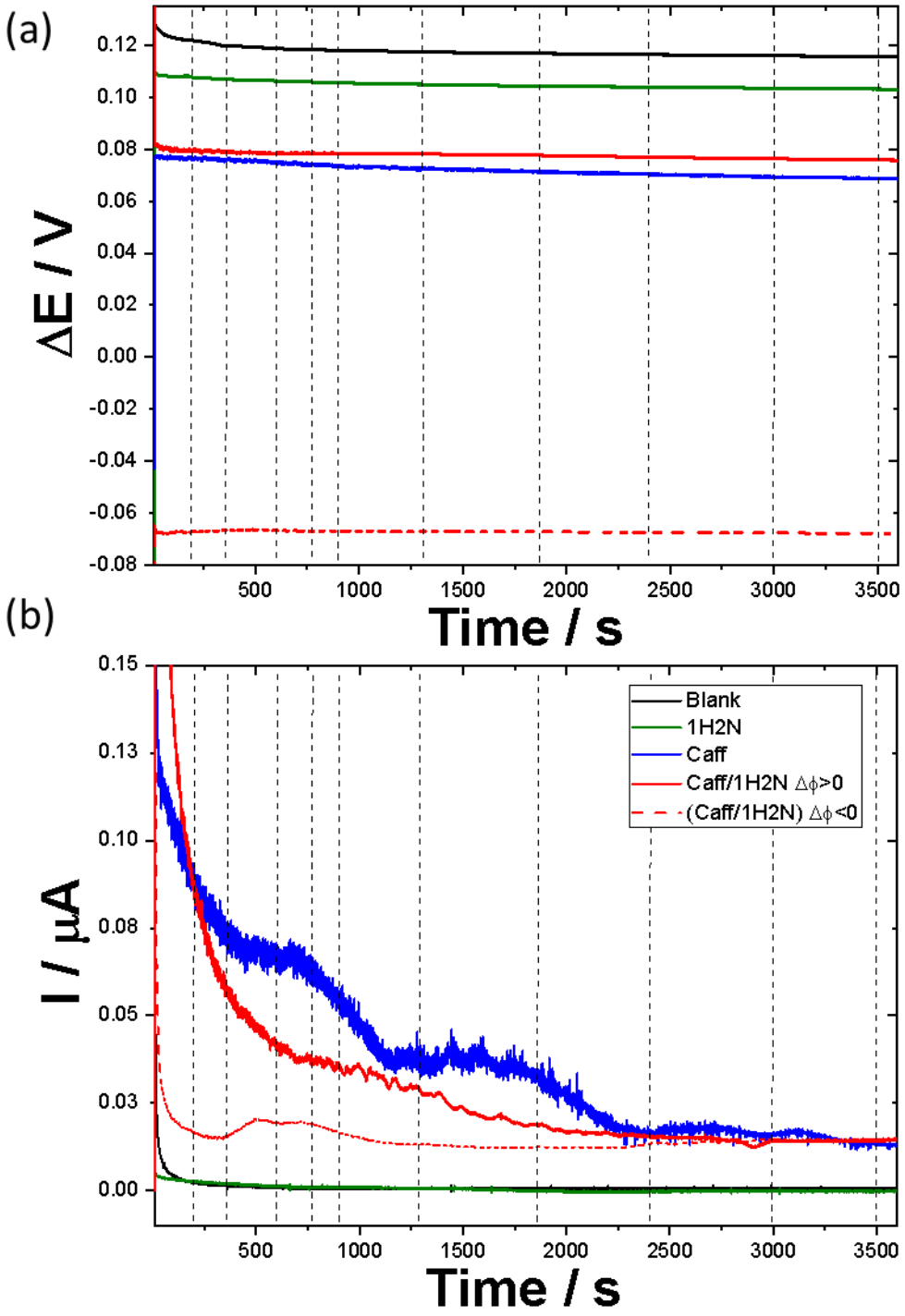

Figure 4: Variation of (a) potential and (b) current as a function of time for the various electrochemical cell 2 configurations. $\frac{c^{o}_{TMA^+}}{c^{w}_{TMA^+}} = \frac{10\ mM}{0.01\ mM}$. Blank: absence of Caff and 1H2N (——), 1H2N: absence of Caff and presence of 1H2N (——), Caff: presence of Caff and absence of 1H2N (——), and Caff/1H2N: presence of Caff and 1H2N (——). Dotted lines represent the times for which I_{rms} and the low frequency noise impedance were calculated.

In Figure 4a, we observe the differences between four experiments: blank (black line, both caffeine and 1H2N are absent from the cell), when only 1H2N was present in the cell (green line), when only caffeine is present in the cell (blue line), and finally when both are present (red line). For the blank electrochemical cell, the potential difference is lower than expected by theory. This might be due to experimental conditions, which do not verify the conditions of Eq.(9). The potential signals exhibit a gradual decrease in all cases. In the Caff/1H2N configuration, we are able to follow the potential changes in the potential during the cocrystallisation process. At this ratio of $\frac{c^o_{TMA^+}}{c^w_{TMA^+}} = \frac{10\ mM}{0.01\ mM}$ and saturated concentration of caffeine we could establish positive potential for the transfer of caffeine. The conditions are sufficient to transfer the caffeine and the formation of cocrystals at the interface is observed. The presence of caffeine has a significant effect on potential. At pH 2, caffeine is present in its cationic form[34] so it is being exchanged with TMA^+ present in the organic phase. The drop in the potential indicate the transfer of caffeine from aqueous phase to the DCE and lowering of the ratio $\frac{c^o_{TMA^+}}{c^w_{TMA^+}}$. The potential in the presence of caffeine (red and blue line) is noisier and corresponds to the exchange of cations ($Caff^+$ and TMA^+) which takes place at the ITIES. The potential of the cell with the presence of only 1H2N comparing with blank is lower due to the presence of H^+ and the facilitated proton transfer. The results shown in Figure 4 are carried out according to Table 1 of cell 2. Here, the pH is equal to 2 and was fixed by adding 10 mM HCl.

Potential variation is concomitant with changes in current, as shown to Figure 4b. The current signals is close to zero for the cells where there is no caffeine, which indicates that no ion transfer is occurring at the ITIES. It can be seen that there is no difference when 1H2N is absent (Figure 4b, black line) and present in the system (green line) which confirms that the 1H2N is not transferring at ITIES[31]. However, when caffeine is present in the aqueous phase, a high initial value for current is observed followed by a significant drop with time. The cocrystals are created after 1 minute, which corresponds to the change in current (Figure 4b red line). This higher current value is attributed to the transfer of caffeine from the aqueous to the organic phase. In the cell with both caffeine and 1H2N present (Fig 4b red line), the current decreases over time. The slope is sharp at the beginning and gradually decreases after 900 s until 2000 s, until it reaches a plateau.

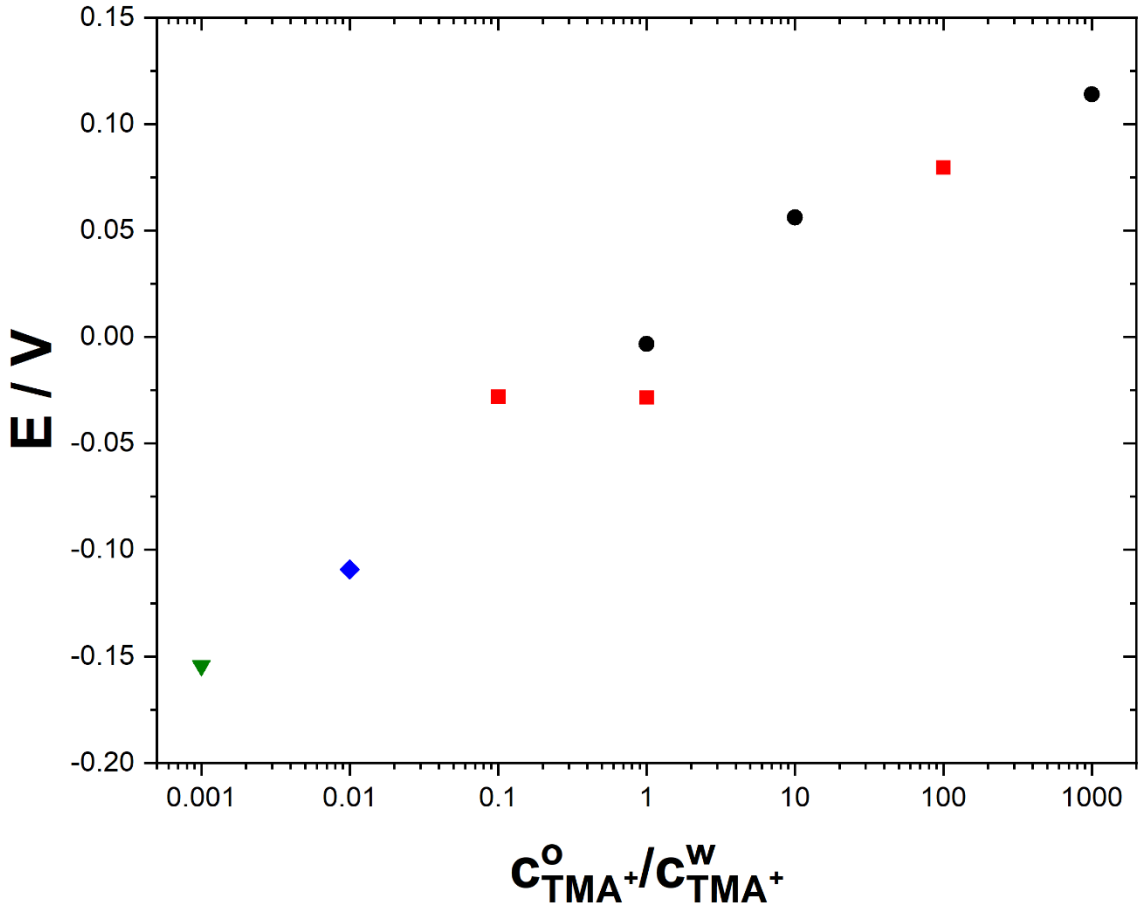

Figure 5: Equilibrium potential based on the ratio $\frac{c^o_{TMA^+}}{c^w_{TMA^+}}$ of electrochemical cell 3 and Caff = 40 mM prepared in the presence of caffeine and 1H2N in the range of time 3000-3600 s. The error bars are shorter than the size of the symbols. The ratio was change by varying the concentration of $c^o_{TMA^+}$. $c^o_{TMA^+}$= 0.01 mM (▼), $c^o_{TMA^+}$= 0.1 mM (♦), $c^o_{TMA^+}$= 1 mM (■), $c^o_{TMA^+}$= 10 mM (●).

These experiments were followed by the series of experiment with various ratio of $\frac{c^o_{TMA^+}}{c^w_{TMA^+}}$ when aqueous solution of caffeine and organic solution of 1H2N were placed together according to electrochemical cell 3. We can observe in Figure 5 that the potential values become higher when we increase the ratio $\frac{c^o_{TMA^+}}{c^w_{TMA^+}}$. With a lower ratio, less caffeine is transferred into the organic phase and less TMA^+ ions transfer to the aqueous phase due to the obtained distribution at the ITIES. It is remarkable that the values of potential are similar for the same ratio $\frac{c^o_{TMA^+}}{c^w_{TMA^+}}$. This is because the changes in the potential do not depend on the concentration of TMA^+ in the organic phase ($c^o_{TMA^+}$) but solely on the ratio $\frac{c^o_{TMA^+}}{c^w_{TMA^+}}$ as indicated in Eq. (8).

Figure 6 shows the I_{rms} (calculated from the results shown in Figure 4b) for the different experimental conditions at various times. For these experiments, the interface is polarised positively. When no caffeine is present (green and black curves on Figure 6), I_{rms} values are below 0.005 µA for the whole duration of the experiment, suggesting that no interfacial charge transfer is occurring. When caffeine is present in the aqueous phase, I_{rms} values are higher, whether 1H2N is present (red curve) or not (blue curve) in the organic phase. In the presence of 1H2N, I_{rms} values decrease faster with time. Indeed, after 1250 s, the I_{rms} values reach the same level as for the control experiments, while it takes 3000 s in the absence of 1H2N. As a control experiment, the current and potential were measured in the presence of both caffeine and 1H2N but when the interfacial potential is negative (Figure S1), which is unfavourable to the formation of caffeine:1H2N cocrystals.[31] I_{rms} values in these experimental conditions are similar to the ones observed in the absence of caffeine confirming that the high I_{rms} values are linked to caffeine charge transfer, when the interface potential is positive.

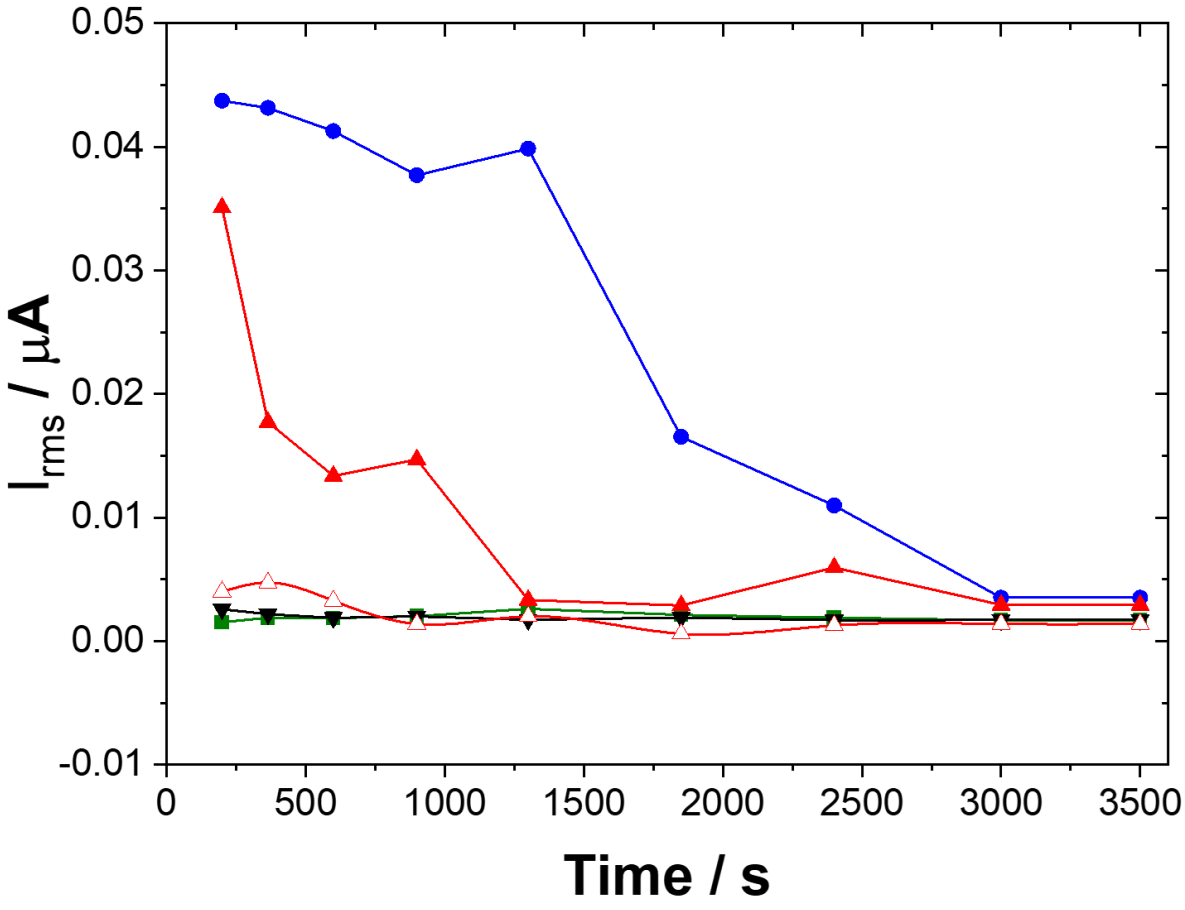

Figure 6: Root mean square of PSD_I. Experimental conditions were: absence of Caff and 1H2N (▼); absence of Caff and presence of 1H2N (■); presence of Caff and absence of 1H2N (●); presence of Caff

and 1H2N (▲ and Δ). Full symbols represent data collected with positive interfacial potential. Interface potential was negative for hollow symbols. $\frac{c^{o}_{TMA^+}}{c^{w}_{TMA^+}} = 1000$

When the experimental conditions for cocrystallisation are met, the low frequency noise impedance decreases within first 1000 s, which can be attributed to the creation of the complex Caff/1H2N (Fig 7 red line) and low current noise. After 1000 s, the R_{sn} flattens, which may be related to the absorption of Caff:1H2N complex at the ITIES. In contrast to a cell in which the complex is not formed (Fig. 7 blue line), the change in the R_{sn} is not significant during the course of an experiment.

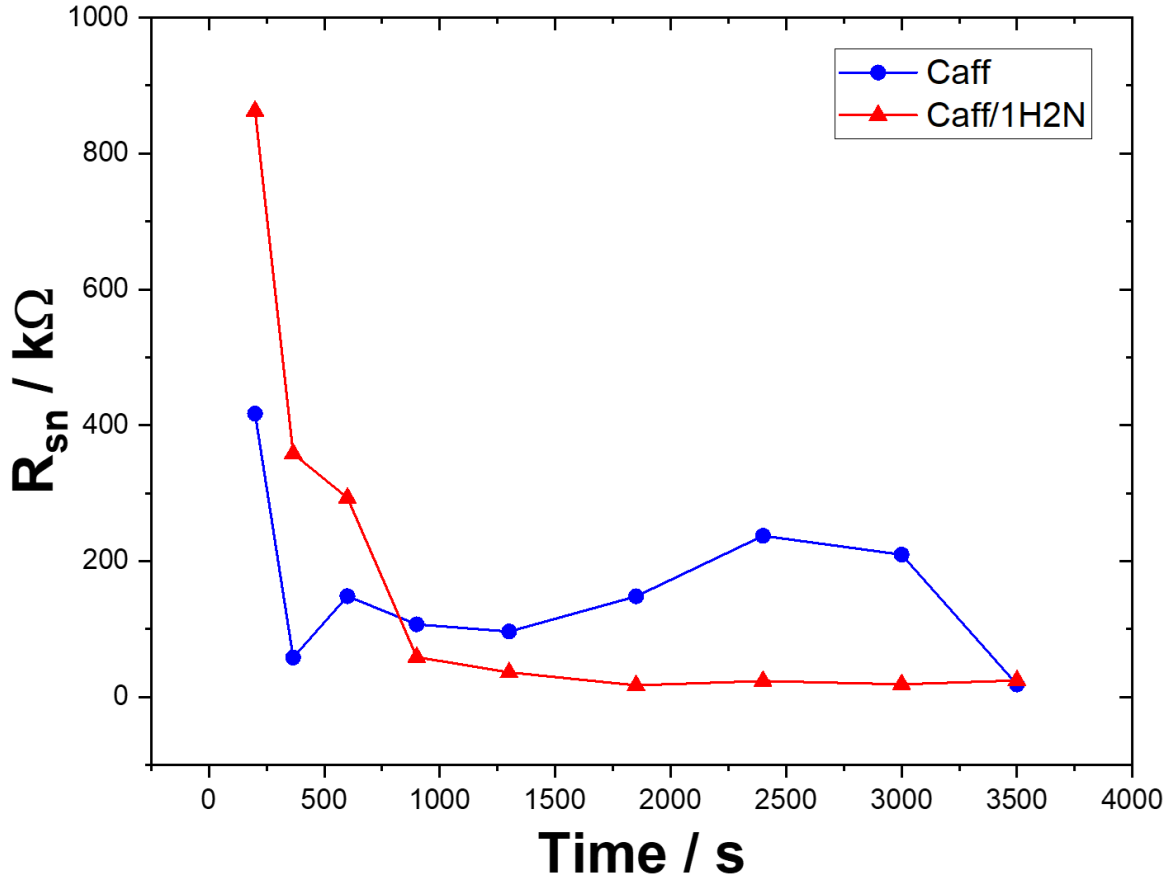

Figure 7: The low frequency noise impedance calculated for electrochemical cell 2 in the absence (●) and in the presence (▲) of 1H2N. Caffeine is present for both experiments.

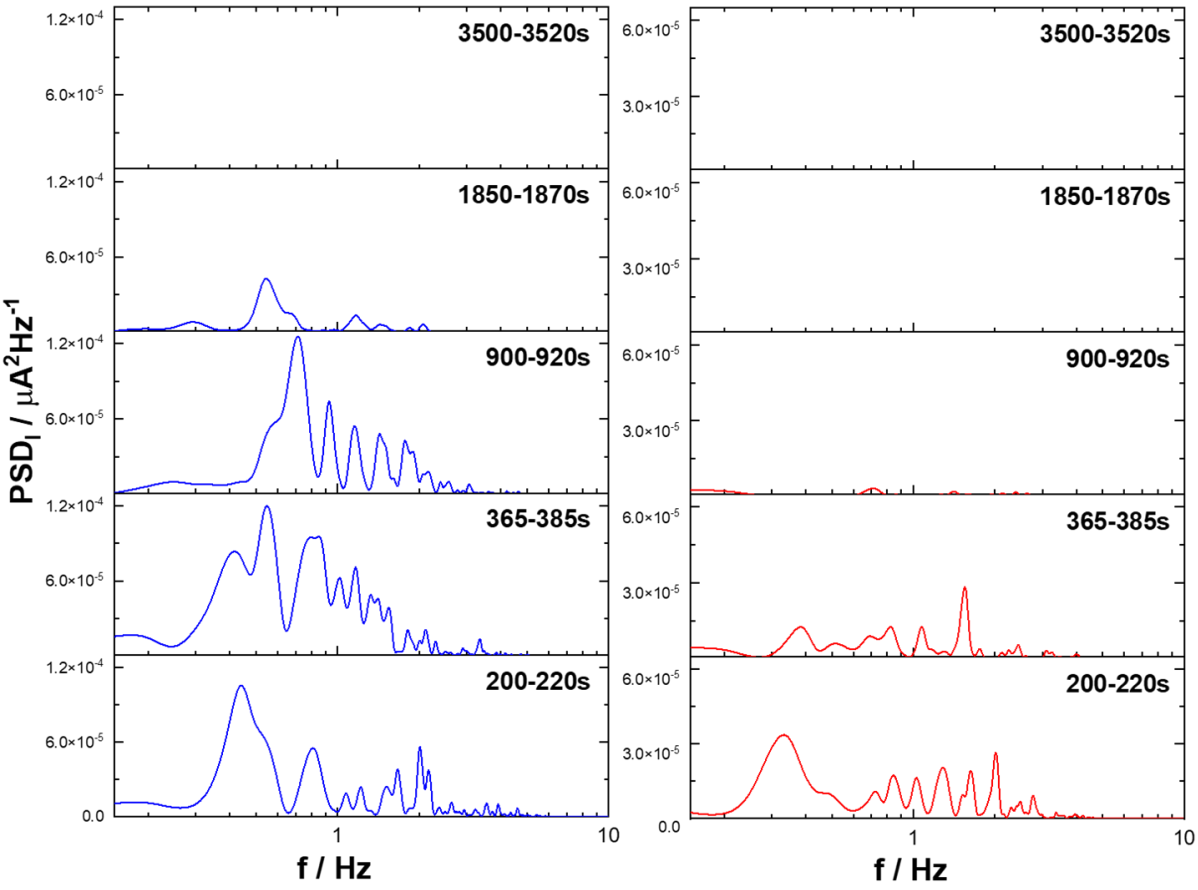

Figure 8: PSD spectra of electrochemical current (PSD_I) recorded in the cell (left) in the absence and (right) in the presence of 1H2N (electrochemical cell 3) calculated from different times.

Figure 8 presents the comparison of PSD_I as the function of frequency in the absence and in the presence of 1H2N; caffeine is present in both experiments. In the absence of 1H2N, the PSD_I values are high and for the times: 200, 365 and 900 s they reach values of 1.2×10^{-4} μA^2 Hz^{-1} and the signal decreased at 1850s. In the presence of both caffeine and 1H2N, cocrystals are formed at the ITIES. The PSD_I values when cocrystals are formed are one order of magnitude lower (4×10^{-5} μA^2 Hz^{-1}) from the beginning of the experiment and is no longer visible after 900 s. Most of the current is cumulated in the region around 1 Hz. However, PSD_I for the formation of crystals appear at slightly lower frequencies than in the sole presence of caffeine. This is due to the complex formation causing the changes at the ITIES which hold caffeine transfer. The signal fades out more rapidly (385 s) upon cocrystal formation as the caffeine enters into a reaction with 1H2N and their adsorption at ITIES. In contrast, in the absence of 1H2N, caffeine continues to transfer to the organic phase as the signal becomes less intense after 1870 s. The PSD spectrum of electrochemical current is much less intense (1×10^{-6} μA^2

Hz^{-1}) when a negative potential is applied, although both Caff and 1H2N (Figure S2) are present in the cell. In such conditions, no formation of cocrystals occurred suggesting that caffeine transfer is responsible for the PSD current.

Caffeine is a weak base with a pK_a of 10.4[35], so it is in cationic form in the acidic conditions (pH = 2) at which the cocrystallisation process occurs.[31] As control experiments, experiments were carried out at pH values of 6 and 11. Caffeine transfers at $\Delta_o^w\phi_{Caffeine}^0 = 0.390\ V$ at pH 2 as shown by the transfer peak observed (Figure S3). However, caffeine transfer was not observed for pH 6 and 11 as it could be masked by the transfer of background electrolyte. Electrochemical noise was also measured at pH 6 and 11 and the PSD_I at various pHs are shown in Figure S4 for the time period 900 - 920 s. At pH 2 and 6, power spectra showed noise with a frequency in the 0.1-10 Hz, whereas the PSD signal was significantly lower at pH 11 in the same frequency region. These observations are consistent with the fact that cocrystals were collected in electrochemical cells at pH 2 and 6 and not at pH 11.

Electrochemical noise analysis shows that, when both caffeine and 1H2N are initially present, interfacial processes of charge transfer are occuring in the first 1000 s of the experiment. During this period, caffeine is transferred across the interface and forms complexes with 1H2N in the organic phase, which then lead to the adsorption of cocrystals at the interface. After 1000 s, electrochemical noise analysis indicates that interfacial charge transfers have ceased, suggesting the cocrystallisation is a two-step process with (i) a potential-driven nucleation with the tranfer of caffeine from the aqueous to the organic phase; (ii) a growth stage where the interfacial potential does no longer play a role.

Conclusion

The potential for the designed electrochemical cells with various ratio of concentration of tetraalkylammonium salts in organic and aqueous phase was monitored. It was found to be in good agreement with the theoretical values based on the Nernst-like equation. The results were similar for three ions: tetramethylammonium, tetraethylammonium and tetrapropylammonium, which indicated that the potential values depend uniquely on the ratio $\frac{c_{TAA+}^o}{c_{TAA+}^w}$. Thus, by varying the ratio of concentrations of the selected ion in the organic and aqueous phases, we were able to obtain suitable potential values to drive the cocrystallisation process. Addition of caffeine and 1-hydroxy-2-naphthoic acid to these well-defined electrochemical cells allowed to monitor

the potential and current at the ITIES. Analysis of the electrochemical current noise showed a clear difference between cells in which cocrystals are formed and those in which cocrystallisation is hindered, either by a negative potential or by a change in pH. Caffeine transfer and cocrystal formation generate different signals with current maxima at frequencies in the 0.1 – 1 Hz range. The EC method is a powerful tool to follow the changes occurring at ITIES in common ion experiments by simultaneous measurement of potential and current.

Acknowledgements

This work was partly supported by the French PIA project “Lorraine Université d'excellence” (reference N° ANR-IDEX-04-LUE) and by the CNRS International Emerging Actions (IEA) program. MK is grateful to Université de Lorraine for funding her PhD.

Keywords: biphasic systems; cocrystallisation; common ion; Electrochemical noise; ITIES.

References

[1] D. P. August, R. A. W. Dryfe, S. J. Haigh, P. R. C. Kent, D. A. Leigh, J. F. Lemonnier, Z. Li, C. A. Muryn, L. I. Palmer, Y. Song, G. F. S. Whitehead, R. J. Young, *Nature* **2020**, *588*, 429–435.

[2] M. D. Scanlon, E. Smirnov, T. J. Stockmann, P. Peljo, *Chem. Rev.* **2018**, *118*, 3722–3751.

[3] E. Smirnov, P. Peljo, H. H. Girault, *Chem. Commun.* **2017**, *53*, 4108–4111.

[4] T. J. Stockmann, J. M. Noël, A. Abou-Hassan, C. Combellas, F. Kanoufi, *J. Phys. Chem. C* **2016**, *120*, 11977–11983.

[5] L. Poltorak, G. Herzog, A. Walcarius, *Langmuir* **2014**, *30*, 11453–11463.

[6] A. F. Molina-Osorio, D. Cheung, C. O’Dwyer, A. A. Stewart, M. Dossot, G. Herzog, M. D. Scanlon, *J. Phys. Chem. C* **2020**, *124*, 6929–6937.

[7] I. Robayo-Molina, A. F. Molina-Osorio, L. Guinane, S. A. M. Tofail, M. D. Scanlon, *J.*

Am. Chem. Soc. **2021**, *143*, 9060–9069.

[8] A. Gamero-Quijano, S. Bhattacharya, P.-A. Cazade, A. F. Molina-Osorio, C. Beecher, A. Djeghader, T. Soulimane, M. Dossot, D. Thompson, G. Herzog, M. D. Scanlon, *Sci. Adv.* **2021**, *7*, eabg4119.

[9] K. Kowalewska, K. Sipa, A. Leniart, S. Skrzypek, L. Poltorak, *Electrochem. Commun.* **2020**, *115*, 106732.

[10] P. Vanýsek, L. B. Ramírez, *J. Chil. Chem. Soc.* **2008**, *53*, 1455–1463.

[11] D. W. M. Arrigan, E. A. De Eulate, Y. Liu, *Aust. J. Chem.* **2016**, *69*, 1016–1032.

[12] Z. Samec, *Pure Appl. Chem.* **2004**, *76*, 2147–2180.

[13] R. A. Hartvig, M. A. Méndez, M. Van De Weert, L. Jorgensen, J. Østergaard, H. H. Girault, H. Jensen, *Anal. Chem.* **2010**, *82*, 7699–7705.

[14] A. Berduque, D. W. M. Arrigan, *Anal. Chem.* **2006**, *78*, 2717–2725.

[15] G. Luo, S. Malkova, J. Yoon, D. G. Schultz, B. Lin, M. Meron, I. Benjamin, P. Vanýsek, M. L. Schlossman, *J. Electroanal. Chem.* **2006**, *593*, 142–158.

[16] F. Li, M. Edwards, J. Guo, P. R. Unwin, *J. Phys. Chem. C* **2009**, *113*, 3553–3565.

[17] P. Peljo, L. Murtomäki, T. Kallio, H. J. Xu, M. Meyer, C. P. Gros, J. M. Barbe, H. H. Girault, K. Laasonen, K. Kontturi, *J. Am. Chem. Soc.* **2012**, *134*, 5974–5984.

[18] L. Rivier, T. J. Stockmann, M. A. Méndez, M. D. Scanlon, P. Peljo, M. Opallo, H. H. Girault, *J. Phys. Chem. C* **2015**, *119*, 25761–25769.

[19] R. Partovi-Nia, B. Su, M. A. Méndez, B. Habermeyer, C. P. Gros, J. M. Barbe, Z. Samec, H. H. Girault, *ChemPhysChem* **2010**, *11*, 2979–2984.

[20] K. Holub, Z. Samec, V. Mareček, *Electrochim. Acta* **2019**, *306*, 541–548.

[21] A. Trojánek, Z. Samec, V. Mareček, *Electrochim. Acta* **2020**, *361*, 137059.

[22] V. Mareček, *Electrochem. Commun.* **2018**, *88*, 57–60.

[23] E. Laborda, A. Molina, V. F. Espín, F. Martínez-Ortiz, J. García de la Torre, R. G. Compton, *Angew. Chemie - Int. Ed.* **2017**, *56*, 782–785.

[24] A. Trojánek, V. Mareček, Z. Samec, *Electrochem. Commun.* **2018**, *86*, 113–116.

[25] F. Mansfeld, H. Xiao, *J. Electrochem. Soc.* **1993**, *140*, 2205–2209.

[26] D.-H. Xia, S. Song, Y. Behnamian, W. Hu, Y. F. Cheng, J.-L. Luo, F. Huet, *J. Electrochem. Soc.* **2020**, *167*, 081507.

[27] Y. J. Tan, S. Bailey, B. Kinsella, *Corros. Sci.* **1996**, *38*, 1681–1695.

[28] Z. Li, A. Homborg, Y. Gonzalez-Garcia, A. Kosari, P. Visser, A. Mol, *Electrochim. Acta* **2022**, *426*, 140733.

[29] A. M. Homborg, E. P. M. Van Westing, T. Tinga, G. M. Ferrari, X. Zhang, J. H. W. De Wit, J. M. C. Mol, *Electrochim. Acta* **2014**, *116*, 355–365.

[30] R. A. Cottis, *Corrosion* **2001**, *57*, 265–285.

[31] M. Kaliszczak, P. Durand, E. Wenger, M. Dossot, F. Jones, D. W. M. Arrigan, G. Herzog, *CrystEngComm* **2022**, *24*, 48–51.

[32] I. B. Obot, I. B. Onyeachu, A. Zeino, S. A. Umoren, *J. Adhes. Sci. Technol.* **2019**, *33*, 1453–1496.

[33] S. Barrozo, R. N. Peres, M. J. Witzler, A. V. Benedetti, C. S. Fugivara, *Eclet. Quim.* **2020**, *45*, 71–75.

[34] L. Poltorak, I. Eggink, M. Hoitink, E. J. R. Sudhölter, M. de Puit, *Anal. Chem.* **2018**, *90*, 7428–7433.

[35] A. Karnjanapiboonwong, A. N. Morse, J. D. Maul, T. A. Anderson, *J. Soils Sediments* **2010**, *10*, 1300–1307.

TOC Entry

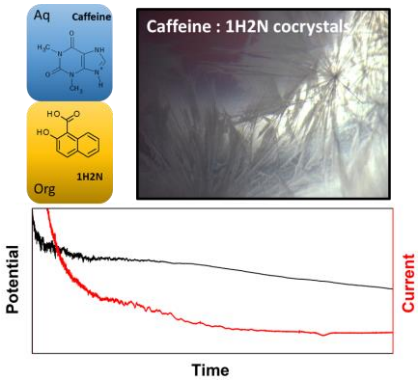

The potential and the current are monitored simulatenously during the cocrystallisation of caffeine and 1H2N at interface between two immiscible electrolyte solutions polarised by a common ion. Electrochemical noise analysis can offer new insights to charge transfer at the ITIES.

Twitter handles:

Magdalena Kaliszczak @kal_magdalena

Franca Jones: @FrancaJones3

Damien Arrigan: @arri_aus

Chemistry at Curtin University: @CurtinChem

Gregoire Herzog: @GregoireHerzog

LCPME: @LCPME_CNRS_UL